

Cyclotron-Resonance-Maser Arrays

Eli Jerby, Amit Kesar, Michael Korol, Li Lei, and Vladimir Dikhtyar

Abstract—The cyclotron-resonance-maser (CRM) array is a radiation source which consists of CRM elements coupled together under a common magnetic field. Each CRM-element employs a low-energy electron-beam which performs a cyclotron interaction with the local electromagnetic wave. These waves can be coupled together among the CRM elements, hence the interaction is coherently synchronized in the entire array. The implementation of the CRM-array approach may alleviate several technological difficulties which impede the development of single-beam gyro-devices. Furthermore, it proposes new features, such as the phased-array antenna incorporated in the CRM-array itself. The CRM-array studies may lead to the development of compact, high-power radiation sources operating at low voltages. This paper introduces new conceptual schemes of CRM-arrays, and presents the progress in related theoretical and experimental studies in our laboratory. These include a multimode analysis of a CRM-array, and a first operation of this device with five carbon-fiber cathodes.

Index Terms—Active antennas, active arrays, cyclotron radiation, cyclotron resonance, masers, microwave generation.

I. INTRODUCTION

HIGH-POWER microwaves (HPM), their generation, and applications, are subjects of great importance in modern science and technology [1]. In particular, gyrotrons [2], [3] and other cyclotron-resonance masers (CRM's) are expected to be widely used as major sources of HPM in future applications in different areas, including material processing, nuclear reactors, radars, accelerators, and others. A comprehensive review on gyrotron and CRM state-of-art is presented in [4].

Gyrotrons, and CRM's in general, have been developed so far mostly as *single* electron-beam devices. The trend toward higher output-powers leads to increase the energy and current of the *sole* electron-beam in gyro-device. Hence, a major part of the *overhead* in such systems is devoted to peripheral accessories needed to maintain the powerful electron-beam itself (the e-gun and collector sections, high-voltage power supplies, insulators, safety shields, etc.). In fact, most of the total length of a typical gyro-device is devoted to this overhead. In addition, a severe difficulty in these high-power levels is caused by the output window [5], which is limited by its power dissipation capabilities.

Several types of microwave tubes with more than one electron-beam (i.e., multibeam tubes) have been proposed and

Manuscript received November 30, 1998; revised December 31, 1998. This work was supported by the Israeli Academy of Science and Humanities under Grant 724/94 ("Multi-beam cyclotron-resonance maser in periodic-waveguide arrays") (1995–1997), by the Israeli Ministries of Energy and Defense and by the Belfer Center of Energy Research.

E. Jerby is with the Faculty of Engineering, Tel Aviv University, Ramat Aviv 69978 Israel (e-mail: jerby@eng.tau.ac.il).

A. Kesar, M. Korol, L. Lei, and V. Dikhtyar are with the Faculty of Engineering, Tel Aviv University, Ramat Aviv 69978 Israel.

Publisher Item Identifier S 0093-3813(99)03375-5.

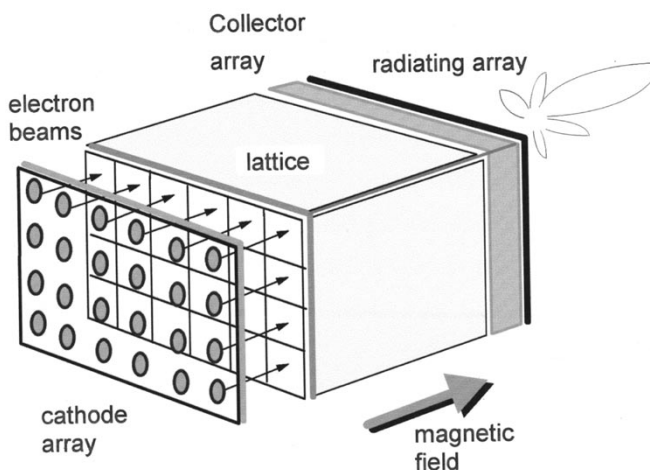


Fig. 1. A conceptual scheme of a CRM-array, including an inherent antenna.

studied by other workers. These include the multiple-beam klystron [6], the cluster klystron for linear colliders [7], the double-stream cyclotron maser [8], and recently the multibeam stagger-tuned gyro-klystrons [9].

The multibeam *CRM-array* concept [10] proposes to increase the CRM output-power by increasing the *number* of interaction channels and electron-beams in the device (rather than the energy of a single beam). This approach incorporates together many single-beam CRM's [i.e., one-dimensional (1-D) devices] into large arrays of two- and three dimensions. Preliminary results of two-dimensional (2-D) CRM-array experiments and some brief conceptual discussions are presented in [11] and [12]. A linear model of a 2-D CRM-array scheme is derived in [13].

The possible use of many low-current, low-energy electron-beams in an array (instead of a single high-current high-energy beam) reduces space-charge and perveance effects, and by synergism, it may increase the total output power and efficiency. The basic components of each CRM-element in the array are relatively simple (smaller e guns, collectors, output windows, etc.), but the entire CRM-array might be regarded as a more complicated system than the single-beam CRM in terms of the electronic circuitry complexity.

An advanced scheme of the CRM-array integrates a phased-array antenna into the device itself [14]. The radiation power is emitted then from the CRM-array directly to the far-field, without any further installation of a separate waveguide toward the (passive) antenna. This CRM-array-antenna integration may simplify the overall radiative system in many applications. Furthermore, the CRM-array may have a unique feature of an *active* phased-array antenna with the ability of radiation steering in space. A schematic illustration of the multibeam CRM-array concept is presented in Fig. 1.

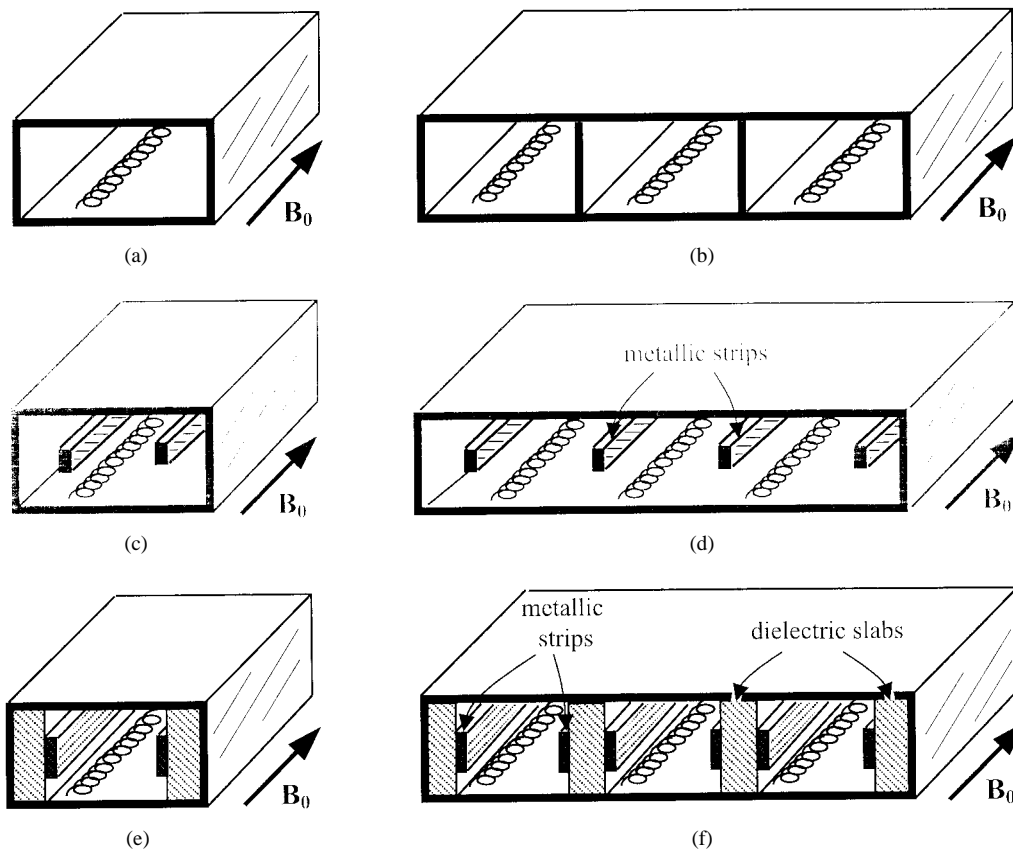


Fig. 2. Nonperiodic CRM's as elements for 2-D CRM-arrays. (a) A rectangular-waveguide CRM [15] and (b) its uncoupled array version. (c) A nondispersive double-stripline CRM [16] and (d) its strongly coupled array. (e) A dielectric-loaded stripline CRM [17] and (f) its array version. In all schemes, B_0 denotes the axial magnetic field in the entire volume.

This paper presents the CRM-array concept comprehensively. It proposes several new CRM-array schemes, and reports on progress in related theoretical and experimental studies toward the development of practical CRM-arrays. The paper is organized as follows; Section II presents new schemes of 2-D and three dimensional (3-D) CRM arrays, in periodic and nonperiodic structures (these are presented as extensions of previously studied 1-D CRM modules). Section III introduces the CRM-array antenna concept with a numerical example of a 33-GHz device. Section IV presents a multimode analysis of a 2-D CRM-array, and Section V shows first experimental results of this device fed by an array of five carbon-fiber cathodes. Section VI concludes the paper with a list of proposed future studies.

II. CRM-ARRAY SCHEMES

The CRM-array consists of many 1-D CRM channels, each operates with a low-voltage, low-perveance electron beam. The different channels may be strongly coupled together through the waveguide lattice. This coupling may enhance synergistic effects, increase the output power further, and/or improve its coherence. (It should be noted, however, that this coupling among the CRM-array elements is not essential in principle. These elements could be independent single-beam CRM amplifiers to which the input signal is divided.) The CRM-array is subjected to a common magnetic field, generated for instance by coils surrounding it. The separate electron

beams are emitted by a cathode array with small kickers attached to each element. Several new conceptual CRM-array schemes are presented.

A. Nonperiodic CRM Arrays

The simplest CRM-element for an array integration is probably the one implemented in a uniform rectangular waveguide, as shown in Fig. 2(a). This elementary CRM device was studied first by Petelin *et al.* [15] in the early 60's. A 2-D-array, proposed on the basis of this element, is shown schematically in Fig. 2(b). In an amplifier scheme, the input signal is divided among the input ports of the CRM elements. The output power can be radiated then directly from the exit plane as an antenna, and combined in the far-field. Alternatively, it can be combined into another waveguide. In an oscillator scheme, coupling holes in the side walls of the adjacent rectangular waveguides may ensure the synchronism and coherence among the CRM-array elements. Similar to the gyrotron, this CRM-array is a narrow-band device.

A widely tunable CRM-array can be constructed on the basis of the double-stripline CRM device shown in Fig. 2(c). This element was studied experimentally in an oscillator scheme and demonstrated a tunability range of more than an octave [16]. A second cyclotron harmonic interaction was observed in this experiment, as well. A CRM-array is proposed on the basis of these elements in a shared *open-space*, as shown in

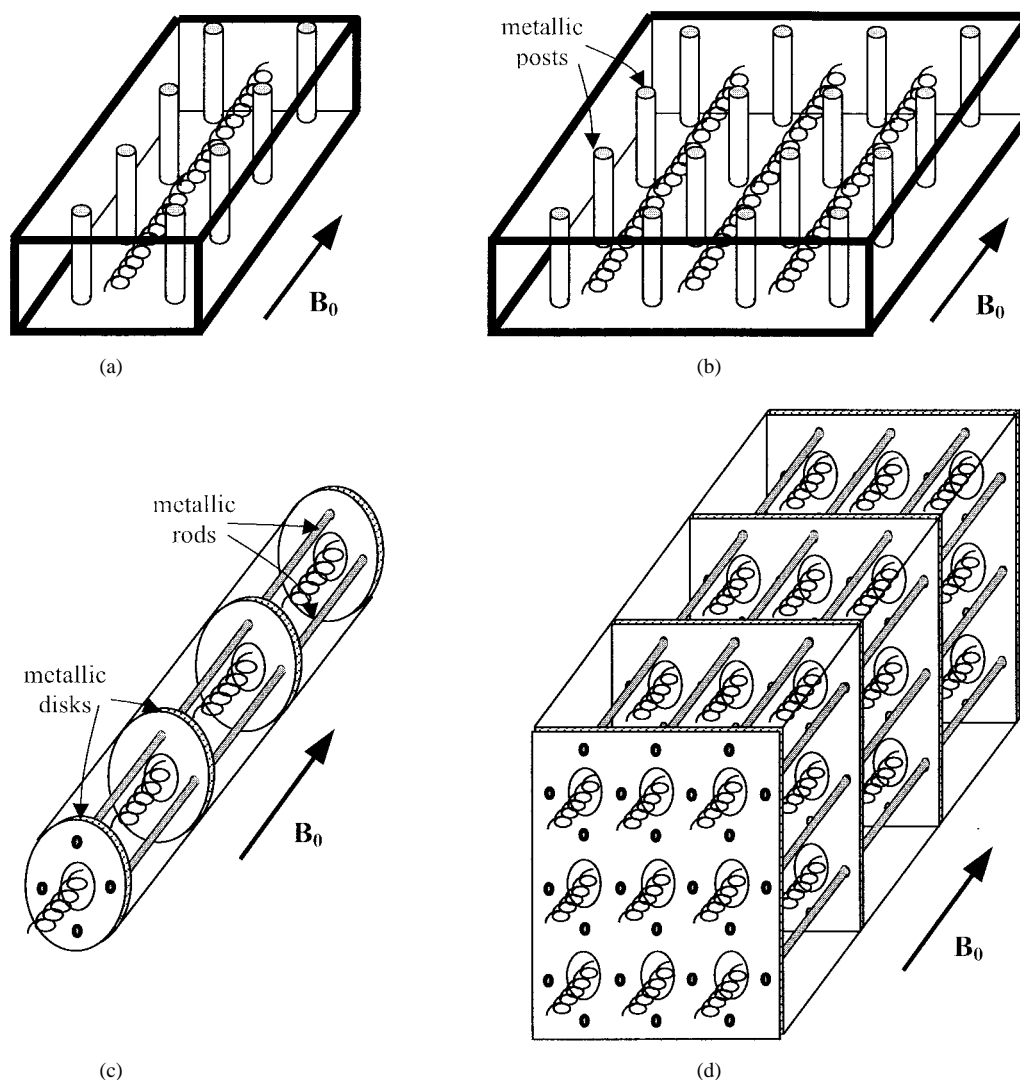


Fig. 3. Periodic CRM's and the corresponding CRM-array schemes. (a) A CRM in a rectangular waveguide loaded by metallic posts. (b) A CRM-array in a 2-D structure of metallic posts. (c) A CRM in a quadrupole waveguide periodically loaded by disks. (d) A 3-D CRM array in a quadrupole lattice.

Fig. 2(d). This CRM-array scheme is characterized by a strong coupling among its elements.

The anomalous Doppler effect was observed in the dielectric-loaded stripline CRM shown in Fig. 2(e) [17], [18]. This effect can be implemented also in a new dielectric-loaded CRM-array, as proposed in Fig. 2(f). As the device shown in Fig. 2(d), this CRM-array is characterized by a strong coupling among its elements, and by a wide tunability range. In addition, it may exhibit a large Doppler up-shift, and an anomalous interaction with initially linear electron beams (i.e., with a zero initial transverse velocity).

B. Periodic CRM-Arrays

The first CRM-arrays presented in [11]–[13] have been developed as 2-D extensions of the periodic-waveguide CRM scheme shown in Fig. 3(a). In the 1-D device, the waveguide includes metal posts in two columns, where the electron-beam flows in between them. This waveguide acts as a bandpass filter (BPF) where the longitudinal distance between adjacent posts (i.e., the waveguide period) is roughly a half-wavelength

of the fundamental frequency, and the transverse distance between the two columns determines the frequency bandwidth. A linear model of CRM interactions with slow and fast waves in this waveguide is presented in [19]. Amplifier [20] and oscillator [21] experiments of this 1-D scheme were conducted at X-band frequencies (8–12 GHz) with electron-beams of ~ 10 keV. The latter experiment yielded a coherent output of a 0.4-kW power at $>25\%$ efficiency. A CRM-array in a 2-D periodic waveguide is presented in Fig. 3(b). In this CRM-array, separate electron beams perform, simultaneously, a cyclotron interaction with a single Bloch wave in the artificial lattice. A theoretical analysis of the CRM-array [13] predicts a considerable gain in a single mode. The mode selectivity and spectral purity in this device stem from the spatial filtering due to the 2-D periodicity. First experimental results are presented in [11] and [12].

Another periodic CRM device which can be extended directly to a 3-D-array is the quadrupole CRM, shown in Fig. 3(c). This periodic structure consists of a quadrupole transmission-line with an array of disks along it, hence, it com-

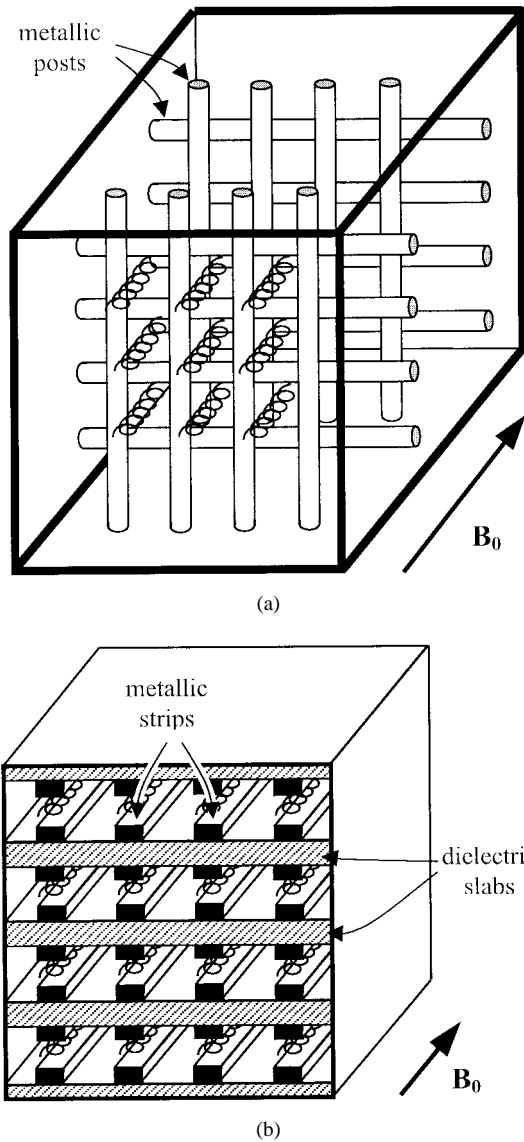


Fig. 4. 3-D CRM-arrays in (a) a lattice of posts and (b) in a stack of dielectric slabs coated by metallic striplines.

bins both azimuthal and axial periodicities. This waveguide supports transverse electro-magnetic (TEM) modes and therefore responds as a BPF with uniformly spaced passbands (i.e., the waveguide period is roughly a multiple half-wavelength at the passband center frequency). This CRM is tuned to operate when the cyclotron harmonic frequencies coincide with the waveguide passbands. In a recent experiment with a tenuous low-energy electron-beam (10 keV, 0.2 A) [22], this device oscillated at the fundamental and high harmonics of the cyclotron frequency. Here, we propose to incorporate single-beam quadrupole CRM elements as *unit-cells* in a 3-D lattice, to form the CRM-array shown in Fig. 3(d). The strong coupling among the elements in this 3-D lattice may excite a CRM interaction with a single Bloch wave.

Other proposals for 3-D CRM arrays are shown in Fig. 4(a) and (b). The first one is a 3-D extension of the periodic-waveguide schemes shown in Fig. 3(a) and (b). It combines two 2-D-arrays in perpendicular directions. These are shifted

by a quarter-wavelength between them to produce circularly polarized waves. (In future schemes, the metallic posts in this artificial lattice can be used also as DC current leads to induce magnetic fields in the entire volume, instead of an external solenoid.) The other 3-D CRM-array shown in Fig. 4(b) is proposed here as a version of the dielectric-loaded stripline CRM-array [Fig. 2(e) and (f)]. Miniature versions of this device can be implemented by methods of microwave-integrated-circuits (MIC). The various elements can be constructed on the same substrate with their peripheral components, such as an input power divider, couplers, and output antenna elements (note that even the cathode array can be “printed” on the same substrate, where the device operates as an array of trochotrons [23]).

III. CRM-ARRAY ANTENNA

The CRM-array presented in Section II might have a useful feature as an active phased-array antenna incorporated in the device itself. The output radiation could be emitted then directly from the exit aperture of the CRM-array, as shown in Fig. 1. The wide cross section of the output aperture may alleviate output-window problems which limit gyrotrons’ output power [5].

In the basic CRM-array antenna scheme, the radiation is emitted from the exit plane to the far-field in a fixed radiation pattern. In more sophisticated schemes, the CRM-array may have features of an active phased-array antenna, in which focusing, steering, and splitting of the radiation lobe are manipulated by varying the voltage profile across the cathode array (as proposed before for free-electron lasers (FEL’s) [24]).

A simplified model for angular steering in a CRM-array antenna is derived in [14]. The concept is demonstrated by the CRM scheme shown in Fig. 2(b). In this example, we assume that the waveguide elements are not coupled together. The device operates here as an array of N amplifiers, where the input signal is equally divided among the CRM elements. The amplitude and phase at the output port of the n th CRM element depend on its physical operating parameters. The Pierce-type gain-dispersion relation which describes the CRM interaction in the linear regime, is written in the form

$$\tilde{A}_n(\hat{s}) = \left[\hat{s} - \left(\hat{s} - \hat{\theta}_n \right)^{-2} \hat{Q}_n(\hat{s}) \right]^{-1} A_0 \quad (1)$$

where A_0 and $\tilde{A}_n(\hat{s})$ are the n th element input and output fields, respectively, \hat{s} denotes the normalized Laplace transform variable, and $\hat{\theta}_n$ is the normalized tuning parameter

$$\hat{\theta}_n = (\omega - \omega_{c,n} - k_z V_{z,n}) \tau_n \quad (2)$$

of the n th element. In (2), ω and k_z are the angular frequency and axial wavenumber of the em-wave in the waveguide, respectively, $V_{z,n}$ and $\omega_{c,n}$ are the axial velocity and the cyclotron frequency of the n th electron beam, respectively, and $\tau_n = L/V_{z,n}$ is the electron time of flight along the interaction region, L . The normalized gain parameter \hat{Q}_n depends on the n th electron beam current and energy, and on other parameters as in [19], for instance.

TABLE I
 NUMERICAL EXAMPLE OF A CRM-ARRAY ANTENNA

Axial magnetic field	B_0	10.5	kG
Frequency	f	32.8	GHz
Electron beam current	I_{eb}	0.8-1.8	A
Electron beam voltage	V_{eb}	14-18	kV
Pitch ratio	V_{\perp}/V_z	1	-
Waveguide width (distance between adjacent elements)	d	3.6	mm
Interaction length	L	0.6	m
Number of elements	N	20	-
Phase difference between adjacent CRM elements	$\Delta\varphi$	0, 30, 60	Deg.
Maximum steering angle	θ_{max}	0, 12, 24	Deg.

For the entire CRM-array antenna, the far-field radiation pattern is approximated by [25]

$$E_{\theta}(\theta) = jk_0 Z_0 \frac{e^{-jk_0 R}}{2\pi R} \sum_{n=1}^N A_n e^{j(nk_x d - \varphi_n)} \int_x E_{x,n} e^{jk_x x} dx \quad (3)$$

where θ is the spatial azimuth angle, A_n and φ_n are the amplitude and phase of the n th CRM-element output, respectively, computed by an inverse Laplace transform of (1). The elements are separated by a distance d in the x direction, $E_{x,n}$ is the electric-field at the n th element aperture (along which the integration is performed), $k_x = k_0 \sin \theta$ is the transverse wavenumber component, R is the radial distance from the antenna, and Z_0 and k_0 are the free-space impedance and wavenumber, respectively. The far-field power density is computed by the Poynting vector $|S| = |E \times H| = Z_0^{-1} |E_{\theta}|^2$.

The numerical analysis dictates how to control the accelerating voltage and the current of the n th electron beam, V_n and I_n , respectively, in order to synthesize the desired amplitude and phase difference between the CRM elements in the array. A numerical example for a 33-GHz device employs the parameters listed in Table I. Fig. 5 shows the CRM output in a contour plot of amplitude and phase versus the electron-beam current and voltage. This graph is used to synthesize the CRM-element operating conditions, according to the desired amplitude and phase. Fig. 6 shows examples of radiation lobes in different steering conditions for an array of 20 CRM elements. Steering angles of 12° and 24° are obtained for phase shifts of 30° and 60° , respectively, between each two adjacent CRM elements in the array.

CRM-array antennas could be used in various applications, including radars, power beaming, plasma heating, and material processing. Another application of the CRM-array could be

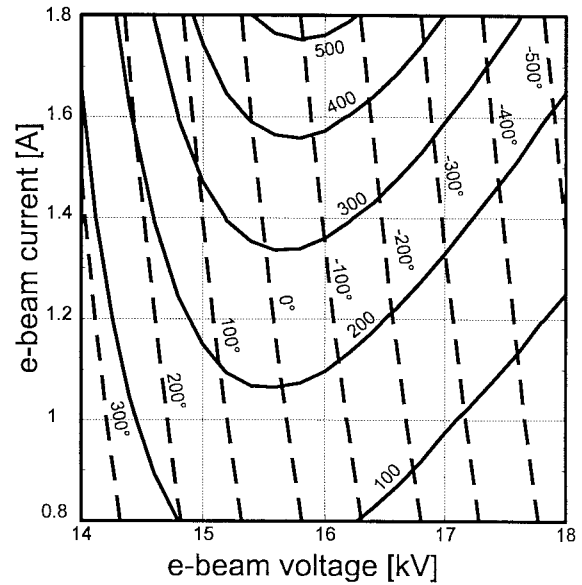


Fig. 5. Gain and phase contours of a single CRM-element for the parameters listed in Table I. The solid and dashed lines are gain and phase contours, respectively, versus the electron-gun voltage and current.

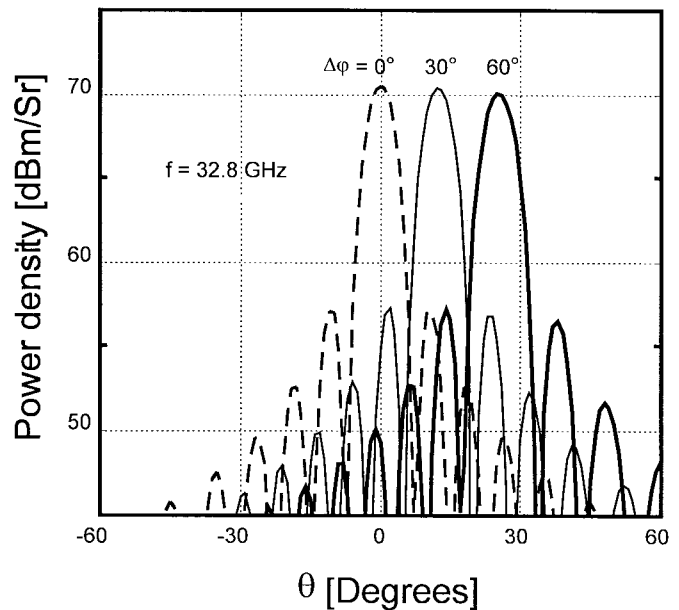


Fig. 6. An angular steering of the 20-element CRM-array (Table I) shown by radiation patterns for phase differences of 0° , 30° , and 60° between the CRM-elements.

as a radiation source integrated in a particle accelerator. The CRM-array may act then as an end-fire near-field antenna, as will be described elsewhere.

IV. COUPLED-MODE CRM-ARRAY ANALYSIS

Unlike the example in Section III, most of the CRM-array schemes presented in Section II involve a strong coupling among their interaction channels. The wide aperture of the array dictates then a multimode CRM interaction. A matrix Pierce-type equation [an extension of the scalar equation (1)] is derived for the analysis of the multimode CRM-array in the

TABLE II
PARAMETERS OF A 2-D CRM-ARRAY EXPERIMENT

<u>Electron beams</u>		
Number of beams	≤5	
Accelerating voltage	~10	kV
Current per beam	~0.25	A
Radius	~2	mm
Pitch ratio (estimate)	<2	
Pulse width	~1	ms
<u>Waveguide parameters</u>		
Total width	69	mm
Height	22	mm
Length	62	cm
Number of posts in a row	6	
Post diameter	2	mm
Transverse periodicity	14	mm
Axial periodicity	30	mm
Number of full periods	20	
Number of half-periods at each end reflector	2	
<u>Axial magnetic field</u>		
Kicker coil	~0.4	kA-turns
Solenoid field	1.8 - 2.8	kG

linear regime. In this analysis, the em wave is expressed as a composition of (periodic) waveguide modes, where each mode is composed of spatial harmonics, as follows:

$$\mathbf{E}(\mathbf{r}) = \sum_{m=1}^{\infty} \left[A_m(z) \sum_{k=-\infty}^{\infty} \mathbf{e}_{mk}(\mathbf{r}_{\perp}) e^{-j\beta_{mk}z} + \hat{z} E_{zm}^{eb}(\mathbf{r}) \right] \quad (4)$$

where m denotes the order of waveguide mode and $A_m(z)$ is its slowly varying amplitude. Each mode of the periodic waveguide is expanded to spatial harmonics, where β_{mk} is the axial wavenumber of the k th spatial harmonic of the m th mode, and \mathbf{e}_{mk} is its transversely dependent vector coefficient. The term E_{zm}^{eb} denotes the axial electrostatic wave in the electron beams, expanded by the membrane functions of the waveguide modes.

A self-consistent set of equations, including the Maxwell, Lorentz, and Vlasov equations, describes the CRM interaction between the Bloch waves and the electron beams. A standard perturbation analysis is applied along the characteristic lines to linearize the system. In this analysis, each electron beam is assumed to be a monoenergetic (cold) beam, but the energy of different beams is not necessarily equal. An integral Laplace transform in the z dimension yields a generalized set of coupled algebraic equations. The derivation results in a matrix

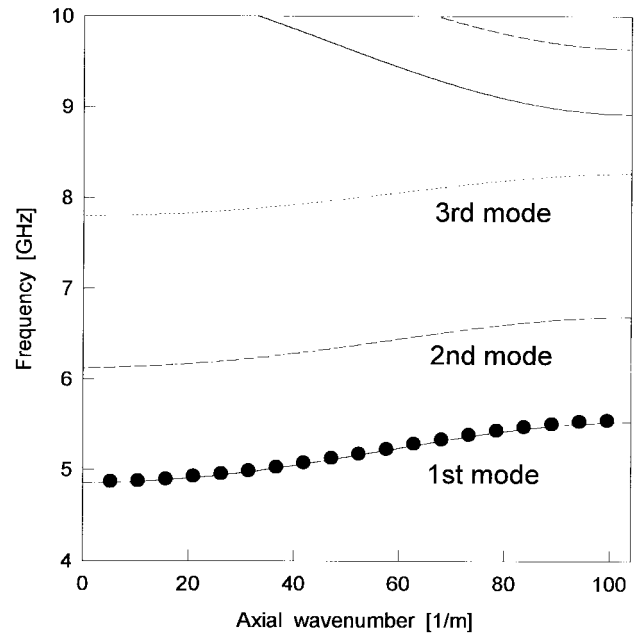


Fig. 7. A Brillouin dispersion diagram of the 2-D periodic waveguide shown in Fig. 3(b) for the parameters listed in Table II. The curves shows theoretical results. The dots are the measurements described in Section V-A.

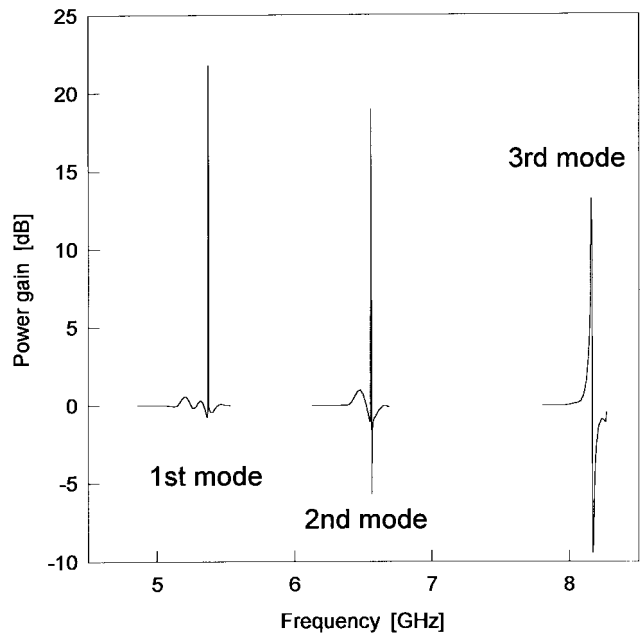


Fig. 8. Gain curves in the first three modes calculated for the CRM-array parameters in Table II.

gain-dispersion equation which describes the evolution of the amplitude and phase of the coupled waveguide modes in the complex Laplace space, as follows:

$$\tilde{\mathbf{A}}(\hat{s}) = \left[\hat{s}\underline{\underline{U}} - \frac{1}{2}\underline{\underline{P}}(\hat{s})^{-1} \sum_{r=1}^{N_r} \left(\hat{s}\underline{\underline{U}} - \hat{\underline{\underline{O}}}_r \right)^{-2} \hat{\underline{\underline{Q}}}_r(\hat{s}) \right]^{-1} \underline{\underline{A}}_0 \quad (5)$$

where the output vector $\tilde{\mathbf{A}}(\hat{s})$ consists of the output signals of the modes $\tilde{A}_m(\hat{s})$. Similarly, the input vector $\underline{\underline{A}}_0$ contains the mode expansion of the input signal, $\underline{\underline{U}}$ denotes the unit

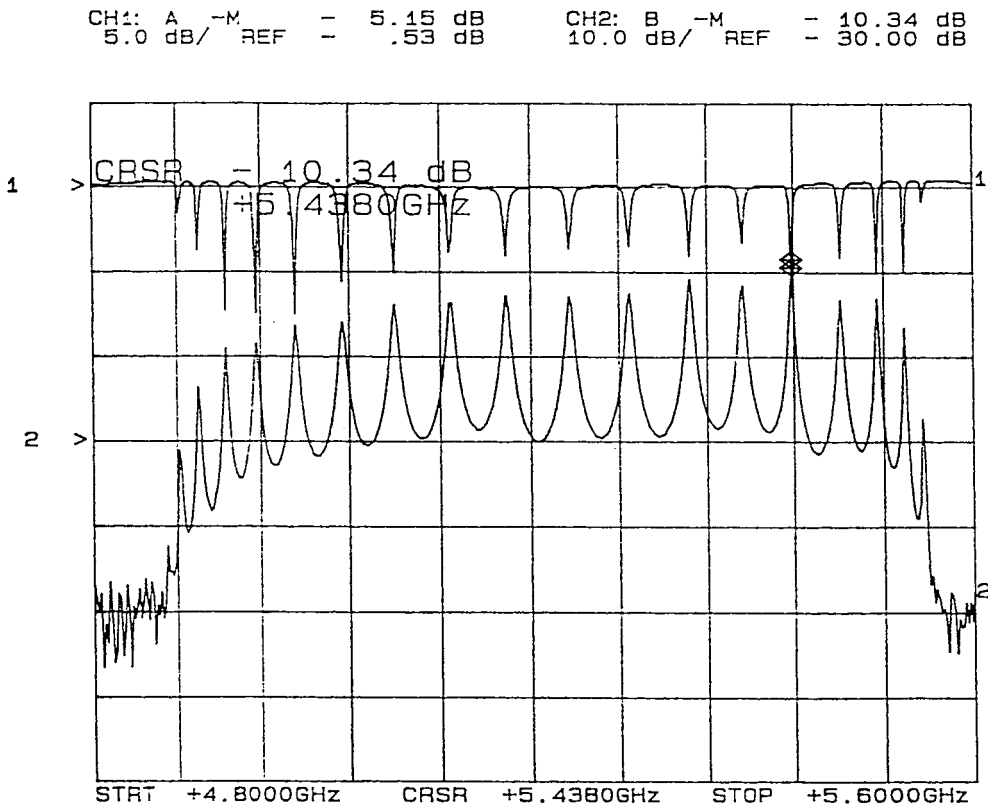


Fig. 9. Reflection and transmission SNA measurements (traces 1 and 2, respectively) of the 2-D periodic waveguide described in Table II.

matrix, $\underline{P}(\hat{s})$ is a matrix which contains the mode powers, and $\hat{\underline{E}}_r$ is a diagonal matrix for the mode tuning with respect to the r th resonance condition [its elements are similar to (2)]. The gain matrix $\hat{\underline{Q}}_r(\hat{s})$ represents the CRM cross-coupling among modes and electron beams, and it depends on the beam currents, energies, and initial transverse velocities.

Equation (5) describes a multiresonance operation of the CRM-array. The sum over N_r different resonances enables, for instance, to let each electron beam a slightly different resonance conditions to widen the gain bandwidth (as studied recently in [9]) or it may describe simultaneous interactions with different modes, etc. The matrix gain-dispersion (5) preserves the form of the scalar Pierce-type equation (1). Its poles describe the shifts of the harmonic wavenumbers β_{mk} in the complex Laplace plane due to the CRM interaction, and the corresponding residues represent their amplitudes.

The solution of (5) is illustrated by a numerical example of a single resonance interaction in the device shown in Fig. 3(b) for the experimental parameters listed in Table II (the experiment is described in Section V). The five electron beams have a circular, transversely uniform cross-section, and they possess the same energy and current. Fig. 7 is a section of the calculated Brillouin diagram which shows the dispersion curves of the first four modes of the 2-D periodic-waveguide, as results from the model derived in [13]. The analysis shows that in a frequency range of one octave, from the fundamental cutoff frequency 4.8 GHz, up to 9.7 GHz, only one mode may propagate in the waveguide at any given frequency. Hence, the waveguide acts as a mode selector at this frequency range. The

single-mode region covers the first passbands of the first three periodic-waveguide modes and partially the second passband of the fundamental mode. The multimode region begins at 9.7 GHz, where the fourth mode intersects with the second passband of the first mode. (The dots on the first passband curve are waveguide measurements described in Section V). Fig. 8 shows the gain calculation results for the CRM-array interaction with five electron beams. Axial magnetic fields of 1.8, 2.25, and 2.85 kG yield interactions with the fundamental harmonics of the first, second, and third modes, respectively.

The theoretical model presented by (5) can be used to analyze CRM-array antennas in which the CRM channels are coupled together, as done in Section III for the uncoupled CRM-array. The limitation on the radiation steering range due to the coupling among the array elements is a subject of a current study.

V. CRM-ARRAY EXPERIMENTS

Several 2-D and 3-D CRM-array schemes are under investigation in our laboratory. The first is the 2-D periodic-waveguide scheme shown in Fig. 3(b). This waveguide was studied before in an array of 4×24 posts, with one and two electron beams emitted by thermionic cathodes. Detailed experimental results obtained by this setup are presented in [12]. More recently, another 2-D CRM-array with 6×20 posts was constructed, with five carbon-fiber emitters. These cold cathodes, operating at low voltages, are simple to use [26], and therefore they are attractive for large-scale CRM arrays. Other type of cathodes studied for the same application are based on ferroelectric materials [27].

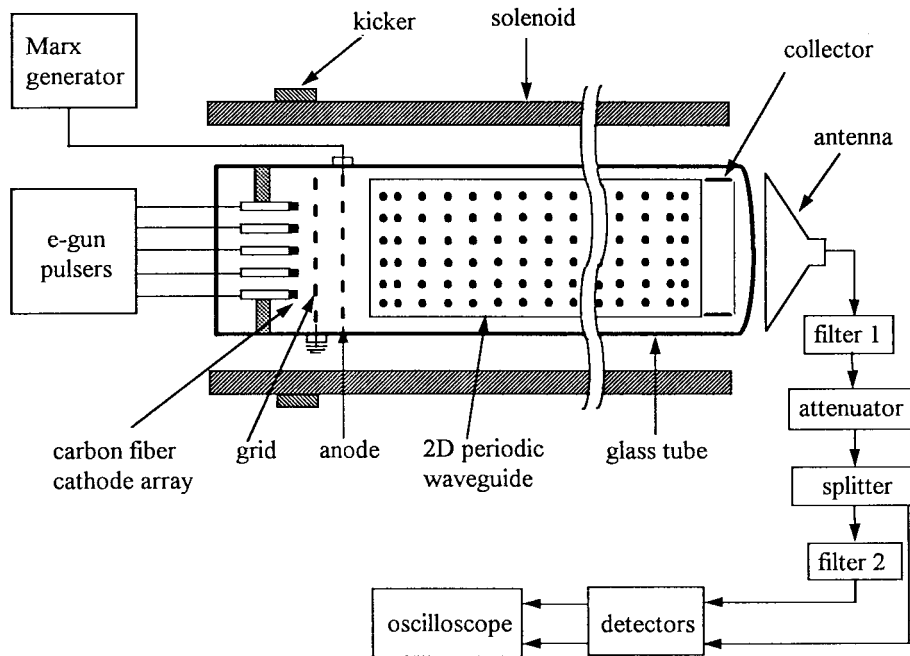


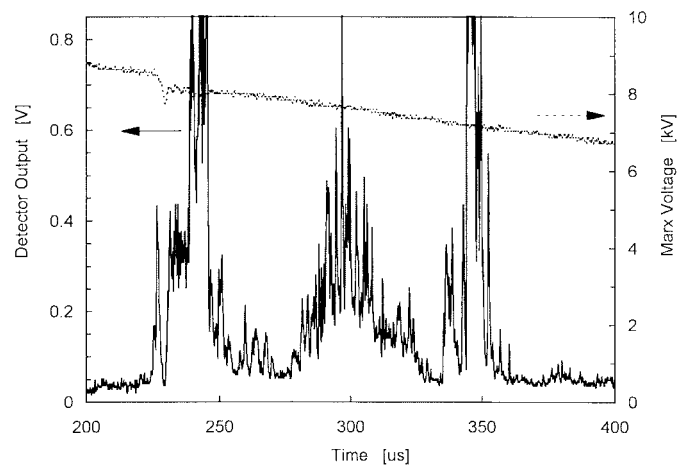
Fig. 10. Experimental setup of the 2-D CRM-array, with the parameters listed in Table II.

TABLE III
PARAMETERS OF A 3-D CRM-ARRAY EXPERIMENT

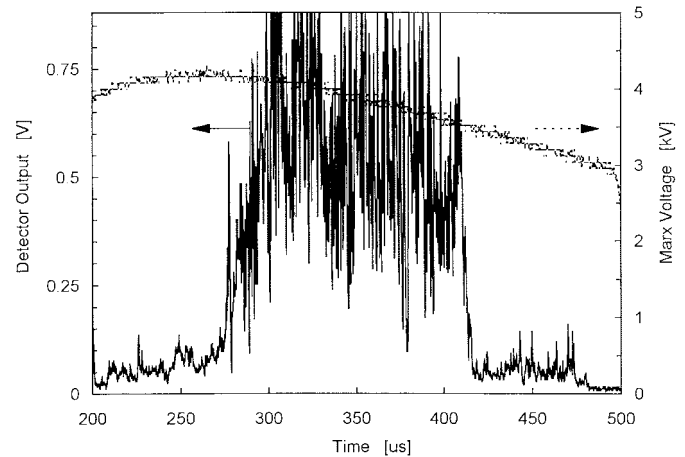
Cavity lattice		
Volume	88 x 88 x 275	mm ³
Number of posts	4 x 4 x 21	
Post diameter	4	mm
Transverse periodicity	18	mm
Axial periodicity	25	mm
Electron beam array		
Number of beams	3 x 3	
Accelerating voltage	< 20	kV
Current per beam	~ 0.2	A
Axial magnetic field		
Helmholtz coils	~ 2.5	kG

A. Cold Waveguide Measurements

The waveguide dispersion diagram shown in Fig. 7 is a key element in the analysis of the CRM-array. An experimental method, similar to [28], is used here to construct the dispersion curve of the 2-D periodic-waveguide shown in Fig. 3(b). This method is based on a set of scalar network-analyzer (SNA) measurements. The waveguide is terminated in these measurements by matched loads, instead of shorts as in [28].



(a)



(b)

Fig. 11. Radiation bursts observed in the 2-D CRM-array experiment, operating with (a) three and (b) five carbon-fiber cathodes.

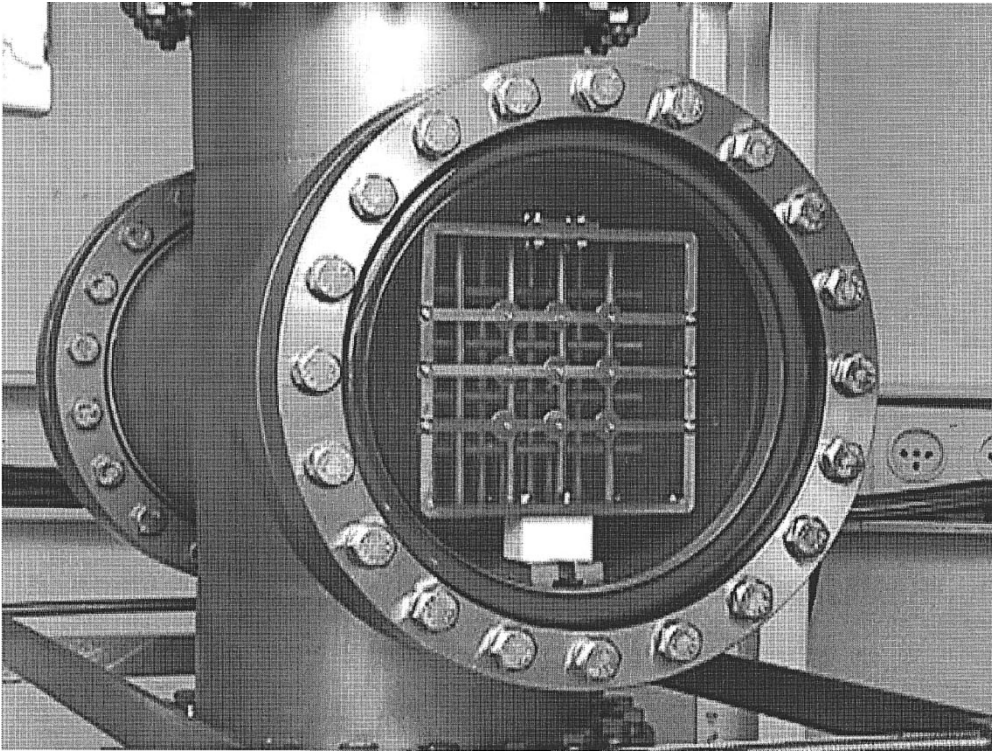


Fig. 12. The 3-D CRM-array experimental device described in Table III.

Fig. 9 shows the SNA reflection and transmission traces of the 2-D waveguide listed in Table II. The reflection and transmission scattering parameters of a finite, lossless periodic-waveguide with N_p axial periods can be written in the form

$$S_{11}^{(N_p)} = \frac{S_{11} \sin \beta_0 N_p p}{\sin \beta_0 N_p p - S_{21} \sin \beta_0 (N_p - 1)p} \quad (6a)$$

$$S_{21}^{(N_p)} = \frac{S_{21} \sin \beta_0 p}{\sin \beta_0 N_p p - S_{21} \sin \beta_0 (N_p - 1)p} \quad (6b)$$

where S_{11} and S_{21} are the reflection and transmission scattering parameters, respectively, of a single period element, β_0 is the fundamental harmonic wavenumber, and p is the period length. The phase shift along one period is $\beta_0 p$, and along the entire waveguide is $N_p \beta_0 p$. The dispersion relation $f(\beta_0)$ shown in Fig. 7 corresponds to an infinitely long waveguide. According to (6a) and (6b), the resonance frequencies of the finite length periodic waveguide satisfy

$$\beta_0(f_r) = \frac{\pi r}{N_p p} \quad (7)$$

where f_r is the r th resonance frequency of the finite waveguide, and $r = 1, 2, \dots, N_p - 1$. Note that in resonance, (6a) and (6b) yield $S_{11}^{(N_p)} = 0$ and $S_{21}^{(N_p)} = 1$, respectively. Hence, the 19 resonances in the SNA reflection and transmission traces in Fig. 9 correspond to the 20 periods of this waveguide. The resonance values of $\beta_0(f_r)$ which result accordingly from Fig. 9 and (7) are marked by 19 dots in Fig. 7. The entire dispersion curve can be interpolated by a cosine series [28], $f(\beta_0) = \sum_{m=0}^M a_m \cos^m \beta_0 p$. For matched terminators the approximation order can be chosen in the range $2 \leq M \leq N_p - 1$. An order of $M = 2$ for

instance, yields an approximated dispersion relation with the coefficients $a_0 = 5.181$, $a_1 = -0.3443$, and $a_2 = 0.0315$. The agreement between this measurement outcome and the theoretical dispersion curve in Fig. 7 is better than 1%.

B. CRM-Array Experimental Setups

The 2-D CRM-array experimental setup is shown in Fig. 10, and its parameters are listed in Table II. The five carbon fiber emitters are driven by negative pulses generated by independent pulsers. The *ignition* of each cathode causes an abrupt fall in its voltage, down to 1 kV during emission. The electrons are emitted toward the grid in a ground potential. The accelerating voltage in the second stage (from the grid to the anode) is provided by a Marx generator. The electron beams are spun up by a kicker, and rotate along the axial solenoid field compensated by Helmholtz coils. The five electron beams, in energies of less than 10 keV, are injected into the corresponding channels in the 2-D periodic waveguide, and interact with the em wave. The periodic waveguide is terminated by half-period reflecting sections in both ends. The output signal is radiated from the exit plane of the waveguide to free-space, and is detected in the near-field by a horn antenna. The output signal is filtered, attenuated, detected, and displayed by the diagnostic setup shown in Fig. 10. Radiation bursts emitted in preliminary experiments by the 2-D CRM-array are shown in Fig. 11(a) and (b), for operations with three and five carbon-fiber cathodes, respectively. A bandpass filter (BPF, 4.7–5.3 GHz) reveals frequency differences between the radiation bursts in Fig. 11(a).

A 3-D CRM-array experiment under construction in our laboratory is based on the scheme shown in Fig. 4(a). The

parameters of this experiment are listed in Table III. The output plane of the 3-D lattice is exposed by a 6-in vacuum window as an antenna aperture shown in Fig. 12. The magnetic field is provided by Helmholtz coils (not shown in Fig. 12). This 3-D CRM-array experiment is intended to demonstrate a CRM-array-antenna with a fixed radiation pattern.

VI. DISCUSSION

The research and development of the CRM-array concept is proceeding in several directions including 1) a conceptual development of new CRM-array schemes, 2) a theoretical modeling of strongly coupled CRM-arrays, 3) development of waveguides and artificial lattices, and methods to measure their dispersion characteristics, 4) studies of cold cathodes made of carbon fibers and ferroelectric plates, and 5) experimental demonstrations of 2-D and 3-D CRM-arrays. The preliminary work presented in this paper should be followed by intensive studies in all these aspects, in order to develop a practical full-scale CRM-array.

The ultimate CRM-array may consist of tens and even hundreds electron-beams, in coupled interaction channels. Its advantages could be 1) a compact size and small system overhead due to the low-voltage and relatively large effective volume, 2) reduced space-charge effects in separated low-current electron beams, 3) improved spectral purity and mode selectivity by the lattice dispersion, and 4) features of active phased-array antenna steered by an electronic phase-control on the electron-beam accelerating voltages.

REFERENCES

- [1] A. V. Gaponov-Grekhov and V. L. Granatstein, *Applications of High-Power Microwaves*. Norwood, MA: Artech House, 1994; and references therein.
- [2] V. A. Flyagin, A. V. Gaponov, M. I. Petelin, and V. K. Yulpatov, "The gyrotron," *IEEE Trans. Microwave Theory Tech.*, vol. MTT-25, pp. 514–521, 1977.
- [3] V. L. Granatstein, "Gyrotron experimental studies," in *High-Power Microwaves*, V. L. Granatstein and I. Alexeff, Eds. Norwood, MA: Artech House, 1987; and references therein.
- [4] M. Thumm, "State of the art of high power gyro-devices and free-electron masers update 1997," Forschungszentrum Karlsruhe, Institut für Technische Physik, Int. Rep., Feb. 1998.
- [5] A. Kasugai, K. Sakamoto, K. Takahashi, M. Tsuneoka, T. Kariya, T. Imai, O. Braz, M. Thumm, J. R. Brandon, R. S. Sussman, A. Beale, "CVD diamond window for high-power and long pulse millimeter wave transmission," *Rev. Sci. Instrum.*, vol. 69, pp. 2160–2165, 1998.
- [6] E. A. Gelvich, L. M. Borisov, Y. V. Zhary, A. D. Zakurdayev, A. S. Pobedonostsev, and V. I. Poognin, "The new generation of high-power multiple-beam klystrons," *IEEE Trans. Microwave Theory Tech.*, vol. 41, pp. 15–19, 1993; and references therein.
- [7] R. B. Palmer, R. C. Fernow, J. Fischer, J. C. Gallardo, H. G. Kirk, S. Ulc, H. Wang, Y. Zhao, K. Eppley, W. Herrmannsfeldt, R. Miller, and D. Yu, "The cluster klystron demonstration experiment," *Nucl. Instrum. Meth. A*, vol. 366, pp. 1–16, 1995.
- [8] G. Bekefi, "Double-stream cyclotron maser," *J. Appl. Phys.*, vol. 71, pp. 4128–4131, 1992.
- [9] G. S. Nusinovich, B. Levush, and B. G. Danly, "Theory of multibeam stagger-tuned gyroklystrons," *IEEE Trans. Plasma Sci.*, vol. 26, pp. 475–481, 1998.
- [10] E. Jerby, M. Korol, L. Lei, V. Dikhtiar, R. Milo, and I. Mastovsky, "Cyclotron-resonance maser arrays—Concept, theory, and experiments," in *Dig. 22 Int. Conf. Infrared Millimeter Waves*, Wintergreen, VA, July 20–25, 1997, pp. 65–66; and references therein.
- [11] L. Lei and E. Jerby, "Cyclotron maser experiment in a two-dimensional array," *SPIE Proc., Intense Microwave Pulses IV*, 1996, vol. 2843, pp. 30–37.
- [12] L. Lei and E. Jerby, "Two-dimensional cyclotron-resonance maser array spectral measurements," *Phys. Rev. E*, vol. 59, pp. 2322–2329, 1999.
- [13] M. Korol and E. Jerby, "Linear analysis of a multibeam cyclotron resonance maser array," *Phys. Rev. E*, vol. 55, pp. 5934–5947, 1997; and references therein.
- [14] A. Kesar and E. Jerby, "Radiation beam steering by a CRM array," in *Proc. Int. Res. Workshop CRM's Gyrotrons*, Ma'ale Hachamisha, Israel, May 18–21, 1998, p. 48.
- [15] M. Petelin, private communication.
- [16] E. Jerby, A. Shahadi, R. Drori, M. Korol, M. Einat, I. Ruvinsky, M. Sheinin, V. Dikhtyar, V. Grinberg, M. Bensal, T. Harhel, Y. Baron, A. Fruchtman, V. L. Granatstein, and G. Bekefi, "Cyclotron resonance maser experiment in a nondispersive waveguide," *IEEE Trans. Plasma Sci.*, vol. 24, pp. 816–824, 1996.
- [17] M. Einat and E. Jerby, "Anomalous and normal Doppler effects in a dielectric-loaded stripline cyclotron resonance masers," *Phys. Rev. E*, vol. 56, pp. 5996–6001, 1997.
- [18] G. Nusinovich, M. Korol, and E. Jerby, "Theory of anomalous-Doppler CRM amplifier with tapered parameters," *Phys. Rev. E*, vol. 59, pp. 2311–2321, Feb. 1999.
- [19] E. Jerby, "Linear analysis of periodic-waveguide cyclotron maser interaction," *Phys. Rev. E*, vol. 49, pp. 4487–4496, 1994.
- [20] E. Jerby and G. Bekefi, "Cyclotron maser experiments in a periodic waveguide," *Phys. Rev. E*, vol. 48, pp. 4637–4641, 1993.
- [21] E. Jerby, A. Shahadi, V. Grinberg, V. Dikhtiar, E. Agmon, H. Golombek, V. Trebich, M. Bensal, and G. Bekefi, "Cyclotron maser oscillator experiments in a periodically loaded waveguide," *IEEE J. Quantum Electron.*, vol. 31, pp. 970–979, 1995.
- [22] Y. Leibovich and E. Jerby, "Cyclotron-resonance maser in a periodically-loaded quadrupole transmission-line," *Phys. Rev. E*, to be published.
- [23] W. Lawson, M. Garven, and G. Nusinovich, "On the design of electron guns for CRM's utilizing trochoidal electron beams," *IEEE Trans. Plasma Sci.*, vol. 24, pp. 999–1004, 1996; and references therein.
- [24] E. Jerby, "Angular steering of the free-electron-laser far-field-radiation beam," *Phys. Rev. A*, vol. 41, pp. 3804–3811, 1990.
- [25] R. E. Collin, *Antennas and Radiowave Propagation*. New York: McGraw Hill, 1985.
- [26] A. Shahadi, E. Jerby, Li Lei, and R. Drori, "Carbon-fiber emitter in a cyclotron-resonance maser experiment," *Nucl. Instrum. Meth.*, vol. A375, pp. 140–142, 1996.
- [27] R. Drori, M. Einat, D. Shur, E. Jerby, G. Rosenman, R. Temkin, R. Advani, and C. Pralong, "Demonstration of microwave generation by a ferroelectric-cathode tube," *Appl. Phys. Lett.*, vol. 74, pp. 335–337, Jan. 1999.
- [28] H. Guo, Y. Carmel, W. R. Lou, L. Chen, J. Rodgers, D. K. Abe, A. Bromborcky, W. Destler, and V. L. Granatstein, "A novel highly accurate synthetic technique for determination of dispersive characteristics in periodic slow wave circuits," *IEEE Trans. Microwave Theory Tech.*, vol. 40, pp. 2086–2094, 1992.

Eli Jerby, for a photograph and biography, see this issue, p. 293.



Amit Kesar received the B.Sc. degree in electrical engineering from Tel Aviv University, Tel Aviv, Israel, in 1997. Currently, he is a graduate student at Tel Aviv University.

His research subject is a three-dimensional multi-beam CRM arrays.



Michael Korol received the M.Sc. degree in physics from Ural State University, Sverdlovsk, USSR, in 1987. He emigrated to Israel in 1991. Currently, he is a Ph.D. degree student at Tel Aviv University, Tel Aviv, Israel.

In his research work, he develops theory for novel cyclotron-resonance maser schemes.



Vladimir Dikhtyar was born in Russia in 1947. He received the M.Sc. degree in radiophysics from the National University of Saratov, Russia, in 1970, and the Ph.D. degree in electrical engineering from the Moscow Institute of Radio Engineering and Electronics of the USSR Academy of Sciences in 1975.

Since then, he was with the Moscow Institute of Radio Engineering and Electronics as a Research Associate. He emigrated to Israel in 1991. Currently, he is a Research Associate at Tel Aviv University, Tel Aviv, Israel. His research interests include waveguide studies and microwave heating of solid materials.



Li Lei received the B.Sc. and M.Sc. degrees in electrical engineering from Huazhong University of Science and Technology, Wuhan, China, in 1985 and 1991, respectively. Currently, she is pursuing the Ph.D. degree and doing experimental research on a multibeam CRM array at Tel Aviv University.